

TABLE DR1. LEE'S FERRY GEOCHRONOLOGY SUMMARY<sup>a</sup>

OSL sample	Deposit <sup>b</sup>	Height (m) <sup>c</sup>	Depth (m)	# Aliquots	Equiv. dose (Gy)	Doserate (Gy/ka)	OSL Age (ka)
USU-122	M2	10.7	3.2	24	76.36 ± 5.32	3.27 ± 0.15	23.4 ± 1.9
USU-131	M3y	12.8	1.0	21	99.70 ± 13.26	2.69 ± 0.12	37.1 ± 4.3
USU-128	J3		1.2	21	142.18 ± 12.15	3.32 ± 0.15	42.9 ± 3.8
USU-127	J3		9.2	20	272.54 ± 20.58	3.67 ± 0.17	74.4 ± 6.4
USU-125	M3	22.2	3.8	21	182.60 ± 14.65	2.44 ± 0.11	74.7 ± 6.4
USU-124	M3	19.2	6.5	21	229.38 ± 13.14	3.00 ± 0.14	76.4 ± 5.9
USU-121	M4	44.1	1.4	30	197.43 ± 17.50	2.05 ± 0.09	96.5 ± 8.6
USU-126	M4	34.9	9.7	29	200.32 ± 18.60	1.92 ± 0.09	104.1 ± 9.7
USU-123	M4	18.3	22	21	141.81 ± 15.72	1.20 ± 0.06	117.8 ± 12.2
USU-130	M5y	45	1.5	21	217.04 ± 21.80	1.74 ± 0.08	125.0 ± 12.0
USU-129	M5	62.5	4.2	20	> 290	2.25 ± 0.10	> 130
USU-787	P2		2	24	54.97 ± 4.30	3.65 ± 0.17	15.2 ± 1.3
USU-786	P2		5	24	68.63 ± 6.74	3.44 ± 0.16	19.9 ± 2.4
USU-784	P3		3	33	80.78 ± 5.81	1.24 ± 0.06	65.7 ± 5.6
USU-785	P3		10	23	96.80 ± 9.37	1.30 ± 0.06	74.8 ± 7.2
USU-783	P4		6	35	128.28 ± 9.23	1.39 ± 0.06	92.4 ± 9.0
USU-782	P5		15	30	118.29 ± 9.65	0.84 ± 0.04	141.5 ± 15.1
TCN sample	Terrace	Height (m)	Prod. rate (atoms/g/a)	Corrected <sup>10</sup> Be conc. (10 <sup>4</sup> atoms/g)	TCN age (ka)		
LF-409	M3	25.6	8.90	33.5 ± 1.1	38.0 ± 4.8		
LF-404s	M4m	41.8	8.93	see item DR3	91.1 +24.9/-11.6		
LF-407	M4o	45.8	9.11	75.1 ± 2.3	84.2 ± 10.8		
LF-410	M5	66.7	9.52	113.9 ± 3.6	123.6 ± 16.0		

<sup>a</sup>see Items DR2 and DR3 for detailed OSL and TCN results, respectively<sup>b</sup>organized by age, "M" is mainstem deposit, "J" is of Johnson Wash, and "P" is of Paria River near its confluence with Colorado

Table DR2. Lee's Ferry OSL Age Information<sup>a</sup>

Sample #	Deposit	Aliquots <sup>b</sup>	Equivalent dose <sup>c</sup> (Gy)	Overdispersion <sup>d</sup> (%)	Dose Rate (Gy/ka)	OSL Age <sup>e</sup> (ka)	
USU-122	M2	24 (33)	76.44 ± 3.78	11.4 ± 1.8	3.27 ± 0.15	23.4	± 1.9
USU-131	M3y	21 (30)	99.97 ± 9.40	20.9 ± 3.4	2.69 ± 0.12	37.1	± 4.3
USU-128	J3	21 (43)	142.33 ± 8.74	12.5 ± 2.4	3.32 ± 0.15	42.9	± 3.8
USU-127	J3	20 (53)	273.56 ± 14.69	9.4 ± 2.3	3.67 ± 0.17	74.4	± 6.4
USU-125	M3	21 (43)	182.54 ± 10.37	12.5 ± 2.1	2.44 ± 0.11	74.7	± 6.4
USU-124	M3	21 (38)	229.31 ± 9.41	8.7 ± 1.5	3.00 ± 0.14	76.4	± 5.9
USU-121	M4	30 (63)	198.04 ± 12.37	16.4 ± 2.3	2.05 ± 0.09	96.5	± 8.6
USU-126	M4	29 (71)	200.25 ± 13.16	17.3 ± 2.4	1.92 ± 0.09	104.1	± 9.7
USU-123	M4	21 (36)	141.59 ± 11.10	17.5 ± 2.8	1.20 ± 0.06	117.8	± 12.2
USU-130	M5y	21 (50)	217.65 ± 15.51	15.7 ± 2.6	1.74 ± 0.08	125.0	± 12.0
USU-129	M5	20 (72)	≥290	13.2 ± 2.3	2.25 ± 0.10	≥130	
USU-787	P2	24 (46)	55.27 ± 2.96	10.7 ± 2.2	3.65 ± 0.17	15.2	± 1.3
USU-786	P2	24 (26)	68.63 ± 6.74	21.8 ± 3.7	3.44 ± 0.16	19.9	± 2.4
USU-784	P3	33 (54)	81.21 ± 4.11	13.2 ± 1.9	1.24 ± 0.06	65.7	± 5.6
USU-785	P3	23 (40)	97.51 ± 6.80	15.0 ± 2.7	1.30 ± 0.06	74.8	± 7.2
USU-783	P4	35 (43)	128.28 ± 9.23	20.6 ± 2.6	1.39 ± 0.06	92.4	± 9.0
USU-782	P5	30 (43)	118.29 ± 9.65	21.8 ± 2.9	0.84 ± 0.04	141.5	± 15.1

<sup>a</sup>Age analysis using the single-aliquot regenerative-dose procedure of Murray and Wintle (2000) on 2-mm small-aliquots of quartz sand utilizing a RISO TL/OSL-DA-20 reader with blue-green light stimulation (470 nm, Hoya U340 filter).

<sup>b</sup>Number of aliquots used in age calculation, with total number of aliquots analyzed in parentheses.

<sup>c</sup>Error on equivalent dose is 2-sigma standard error, calculated using the Central Age Model of Galbraith et al. (1999).

<sup>d</sup>Overdispersion represents scatter in equivalent dose beyond calculated uncertainties in data, values over 20% represent significant scatter.

<sup>e</sup>Error on age is 2-sigma standard error.

Lee's Ferry Dose Rate Information<sup>a</sup>

Sample #	Deposit	Depth (m)	Grain size fraction (µm)	U (ppm) <sup>b</sup>	Th (ppm) <sup>b</sup>	%K <sup>b</sup>	Rb (ppm) <sup>b</sup>	Cosmic (Gy/ka) <sup>c</sup>	Dose Rate (Gy/ka) <sup>d</sup>
USU-122	M2	3.2	90-150	2.8 ± 0.2	10.2 ± 0.9	1.79 ± 0.04	69.2 ± 2.8	0.16 ± 0.02	3.27 ± 0.15
USU-131	M3y	1.0	90-150	2.3 ± 0.2	8.2 ± 0.7	1.41 ± 0.04	49.8 ± 2.0	0.22 ± 0.02	2.69 ± 0.12
USU-128	J3	1.2	63-125	2.3 ± 0.2	6.6 ± 0.6	2.14 ± 0.05	80.3 ± 3.2	0.21 ± 0.02	3.32 ± 0.15
USU-127	J3	9.2	63-125	6.3 ± 0.4	5.2 ± 0.5	1.77 ± 0.04	68.7 ± 2.7	0.08 ± 0.01	3.67 ± 0.17
USU-125	M3	3.8	90-150	2.0 ± 0.1	5.4 ± 0.5	1.49 ± 0.04	58.3 ± 2.3	0.15 ± 0.01	2.44 ± 0.11
USU-124	M3	6.5	90-150	2.9 ± 0.2	8.0 ± 0.7	1.70 ± 0.04	70.5 ± 2.8	0.11 ± 0.01	3.00 ± 0.14
USU-121	M4	1.4	90-150	1.5 ± 0.1	4.2 ± 0.4	1.24 ± 0.03	48.4 ± 1.9	0.20 ± 0.02	2.05 ± 0.09
USU-126	M4	9.7	90-150	1.1 ± 0.1	3.2 ± 0.3	1.41 ± 0.04	52.2 ± 2.1	0.08 ± 0.01	1.92 ± 0.09
USU-123	M4	22	90-150	0.8 ± 0.1	2.5 ± 0.2	0.83 ± 0.02	30.1 ± 1.2	0.03 ± 0.00	1.20 ± 0.06
USU-130	M5y	1.5	90-150	1.7 ± 0.1	3.6 ± 0.3	0.92 ± 0.02	31.8 ± 1.3	0.20 ± 0.02	1.74 ± 0.08
USU-129	M5	4.2	90-150	1.8 ± 0.1	5.0 ± 0.5	1.37 ± 0.03	47.3 ± 1.9	0.14 ± 0.01	2.25 ± 0.10
USU-782	P5	15	90-150	0.7 ± 0.1	2.1 ± 0.2	0.49 ± 0.01	19.2 ± 0.8	0.05 ± 0.00	0.84 ± 0.04
USU-783	P4	6	90-150	1.2 ± 0.1	3.1 ± 0.3	0.80 ± 0.02	30.2 ± 1.2	0.11 ± 0.01	1.39 ± 0.06
USU-784	P3	3	90-150	1.2 ± 0.1	5.2 ± 0.5	0.50 ± 0.01	18.7 ± 0.7	0.11 ± 0.01	1.24 ± 0.06
USU-785	P3	10	90-150	0.9 ± 0.1	3.0 ± 0.3	0.83 ± 0.02	31.0 ± 1.2	0.08 ± 0.01	1.30 ± 0.06
USU-786	P2	5	63-150	3.3 ± 0.2	9.4 ± 0.9	1.92 ± 0.05	81.4 ± 3.3	0.13 ± 0.01	3.44 ± 0.16
USU-787	P2	2	63-125	3.5 ± 0.3	9.6 ± 0.9	1.99 ± 0.05	86.1 ± 3.4	0.19 ± 0.02	3.65 ± 0.17

<sup>a</sup>Radioelemental concentrations by ICP-MS and ICP-AES at ALS Chemex, dose rate using conversion factors in Guérin et al. (2011).

<sup>b</sup>Errors on concentration values are based on detection limits and follow those described in Rittenour et al. (2005).

<sup>c</sup>Contribution of cosmic radiation to dose rate is calculated using sample depth, elevation, and lat/long following Prescott and Hutton (1994).

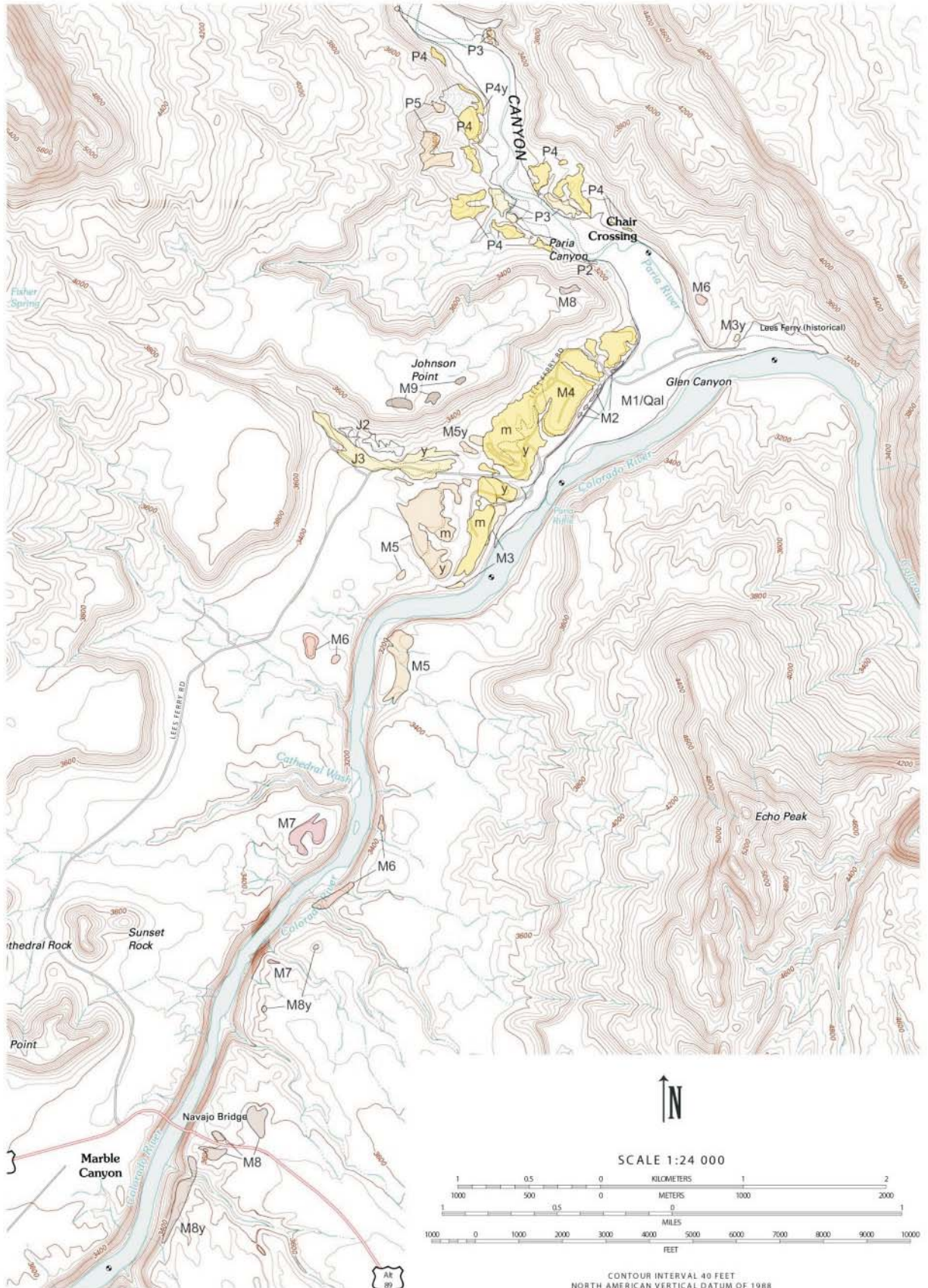
<sup>d</sup>Dose rate was calculated assuming a 2.0 g/cm<sup>3</sup> sample density, 3 ± 3% water content and reported grain size

## REFERENCES CITED

- Galbraith, R.F., Roberts, R.G., Laslett, G.M., Yoshida, H. and Olley, J.M., 1999, Optical dating of single and multiple grains of quartz from Jinnium Rock Shelter, northern Australia: Part I, experimental design and statistical models: *Archaeometry*, v. 41, p. 339-364.
- Guérin, G., Mercier, N., and Adamiec, G., 2011, Dose-rate conversion factors: update: *Ancient TL*. v. 29, p.5-8.
- Murray, A.S. and Wintle, A.G., 2000, Luminescence dating of quartz using an improved single aliquot regenerative-dose protocol. *Radiation Measurements*, v. 32, p. 57-73.
- Prescott, J. R. and Hutton, J.T., 1994, Cosmic ray contributions to dose rates for luminescence and ESR dating: *Radiation Measurements*, v. 23, p. 497-500.
- Rittenour, T.M., Goble, R.J., Blum, M.D., 2005, Development of an OSL chronology for late Pleistocene channel belts in the lower Mississippi valley: *Quaternary Science Reviews*, v.24, p. 2539-2554.

# Data Repository Item: Pleistocene Terrace Deposits of the Lee's Ferry Area

Joel L. Pederson and W. Scott Cragun  
Department of Geology, Utah State University



## Item DR3

Table DR3.1. Lee's Ferry TCN Sample Site Information<sup>a</sup>

Field ID	Latitude	Longitude	Elevation	Altitude correction <sup>b</sup>	Sample thickness	Density	Shielding factor	Depth to sample top
	(d.d)	(d.d)	(m)	(std)	(cm)	(g/cm <sup>3</sup> )	(unit less)	(cm)
GC-04-LF-407	36.859	-111.600	995	std	2	2	0.979	0
GC-04-LF-409	36.854	-111.605	975	std	2	2	0.979	0
GC-04-LF-410	36.850	-111.610	1021	std	2	2	0.979	0
GC-04-LF-404.30s	36.852	-111.606	985	std	5	2.6	0.979	27.5
GC-04-LF-404.60s	36.852	-111.606	985	std	5	2.6	0.979	57.5
GC-04-LF-404.100s	36.852	-111.606	985	std	5	2.6	0.979	97.5
GC-04-LF-404.140s	36.852	-111.606	985	std	5	2.6	0.979	137.5
GC-04-LF-404.180s	36.852	-111.606	985	std	5	2.6	0.979	177.5
GC-04-LF-404.220s	36.852	-111.606	985	std	5	2.6	0.979	217.5

<sup>a</sup>all samples collected in October, 2004

<sup>b</sup>tag used for input into the online CRONUS calculator specifying a standard pressure correction for the elevation (see <http://hess.ess.washington.edu/> for more information)

Table DR3.2. Lee's Ferry TCN AMS Information

Field ID	CNEF ID	Be AMS ID	Qtz Mass	<sup>9</sup> Be added	<sup>10</sup> Be/ <sup>9</sup> Be (boron corr.)	<sup>10</sup> Be/ <sup>9</sup> Be error (1σ)	<sup>10</sup> Be/ <sup>9</sup> Be (normalized) <sup>a</sup>	<sup>10</sup> Be from blank	<sup>10</sup> Be from blank error (1σ)	<sup>10</sup> Be in qtz (blank corr.)
			(g)	(10 <sup>19</sup> atoms)	(x 10 <sup>-13</sup> )	(x 10 <sup>-13</sup> )	(x 10 <sup>-13</sup> )	(10 <sup>4</sup> atoms)	(10 <sup>4</sup> atoms)	(10 <sup>4</sup> atoms)
blank for 1591-1594	1733	BE21502		1.666	0.05992	0.007399	0.05418			
blank for 1595-1600	1537	BE20404		2.006	0.09456	0.009377	0.08550			
GC-04-LF-407	1591	BE21498	20.4978	1.596	12.05	0.2903	10.90	9.026	0.8950	1731
GC-04-LF-409	1593	BE21500	20.4988	1.651	5.947	0.1431	5.377	9.026	0.8950	878.7
GC-04-LF-410	1594	BE21501	20.5037	1.606	17.47	0.4190	15.80	9.026	0.8950	2527
GC-04-LF-404.30s	1595	BE20406	45.2566	2.001	14.04	0.3254	12.69	17.150	2.118	2523
GC-04-LF-404.60s	1596	BE20407	45.9469	1.949	10.49	0.2089	9.484	17.150	2.118	1831
GC-04-LF-404.100s	1597	BE20408	50.1042	2.029	7.919	0.1841	7.160	17.150	2.118	1436
GC-04-LF-404.140s	1598	BE20409	51.1421	1.971	5.807	0.1345	5.251	17.150	2.118	1018
GC-04-LF-404.180s	1599	BE20410	55.3693	2.004	4.803	0.1141	4.343	17.150	2.118	853.4
GC-04-LF-404.220s	1600	BE20411	55.1112	1.932	4.245	0.08794	3.838	17.150	2.118	724.5

<sup>a</sup>ratios normalized to revised standardizations of Nishiizumi et al. (2007); AMS standard KNSTD3110 originally used with all measurements (normalization factor = 0.9042)

Table DR3.3. Lee's Ferry TCN Concentration and Error Information

Field ID	<sup>10</sup> Be in qtz	Assumed <sup>10</sup> Be inheritance <sup>a</sup>	Inh corr. <sup>10</sup> Be	AMS error (1σ)	Chemistry error (1σ)	Blank error (1σ)	TOTAL 1σ PRECISION <sup>b</sup>
	(atom/g)	(atoms/g)	(atoms/g)	(%)	(%)	(%)	(%)
GC-04-LF-407	844317	93300	<b>751017</b>	2.41%	2.00%	0.06%	3.13%
GC-04-LF-409	428678	93300	<b>335378</b>	2.41%	2.00%	0.13%	3.13%
GC-04-LF-410	1232480	93300	<b>1139180</b>	2.40%	2.00%	0.04%	3.12%
GC-04-LF-404.30s	<b>557532</b>			2.32%	2.00%	0.07%	3.06%
GC-04-LF-404.60s	<b>398608</b>			1.99%	2.00%	0.09%	2.82%
GC-04-LF-404.100s	<b>286546</b>			2.33%	2.00%	0.12%	3.07%
GC-04-LF-404.140s	<b>199039</b>			2.32%	2.00%	0.17%	3.06%
GC-04-LF-404.180s	<b>154137</b>			2.38%	2.00%	0.20%	3.11%
GC-04-LF-404.220s	<b>131467</b>			2.07%	2.00%	0.23%	2.89%

<sup>a</sup>inheritance of  $9.33 \times 10^4$  (atoms/g) assumed from simulation of depth profile samples (GC-04-LF-404.##), after Hidy et al. (2010)

<sup>b</sup>total precision calculated by adding AMS, chemistry, and blank errors in quadrature

Table DR3.4. Lee's Ferry TCN Pavement Age Information

Field ID	Erosion Rate	Production rate <sup>a</sup>		Exposure age	Internal	prod rate	Mean Age	Unc (2σ)	Unc (2σ)	Unc (2σ)
		(muons)	(spallation)	(Lal and Stone)	uncertainty	geomagnetic	Geomagnetic	total precision	total error	total error
	(cm/yr)	(atoms/g per yr)	(atoms/g per yr)	(yr)	(yr)	(atoms/g per yr)	(yr)	(%)	(%)	(yr)
GC-04-LF-407	0	0.25	8.61	86596	2771	9.11	<b>84225</b>	6.4%	21%	17686
GC-04-LF-409	0	0.25	8.48	38788	1226	8.90	<b>38041</b>	6.3%	21%	7979
GC-04-LF-410	0	0.25	8.78	130268	4204	9.52	<b>123629</b>	6.5%	21%	25981
GC-04-LF-407	0.00038	0.25	8.61	122964	5969	9.39	<b>116070</b>	9.7%	22%	25804
GC-04-LF-409	0.00038	0.25	8.48	44202	1610	9.01	<b>42831</b>	7.3%	21%	9117
GC-04-LF-410	0.00038	0.25	8.78	259471	21765	10.00	<b>234351</b>	16.8%	26%	61176

<sup>a</sup>production rate is the sum of spallogenic and muonic production from CRONUS Calculator vers. 2.2 (April 10, 2012) computed by averaging the results of all four time-averaged scaling methods (Balco et al., 2008), considering a thickness of 2 cm (for depth profile, thickness of 0 cm) and a shielding factor of 0.979.

Samples: GC-04-LF-404.##		age	inheritance	erosion rate
		(ka)	(10 <sup>4</sup> atoms/g)	(cm/ka)
<b>Lal and Stone</b>	mean	99.1	9.1	0.24
	median	98.6	9.15	0.26
	mode	<b>89.4</b>	9.34	0.39
	min $\chi^2$	83.9	8.36	0.09
	maximum	128.7	10.52	0.5
	minimum	73.8	6.57	0
	Bayesian most probable	<b>94.6</b>	9.32	0.37
	Bayesian 2 $\sigma$ upper	119.2	10.46	0.42
	Bayesian 2 $\sigma$ low er	81.7	7.79	0.03
<b>Geomagnetic</b>	mean	96.4	9.13	0.25
	median	96	9.18	0.26
	mode	<b>86.4</b>	9.42	0.40
	min $\chi^2$	87.3	8.31	0.20
	maximum	125.3	10.53	0.50
	minimum	71.7	6.49	0
	Bayesian most probable	<b>91.1</b>	9.19	0.38
	Bayesian 2 $\sigma$ upper	116	10.48	0.43
	Bayesian 2 $\sigma$ low er	79.5	7.82	0.03

<sup>a</sup>Bayesian output from Hidy et al. (2010) calculator (vers. 1.2), based on 1 million curve fits, using geomagnetic field-corrected production rates, bulk density with stochastic range of 2.2 to 2.5 g/cm<sup>3</sup> as measured in the field, and erosion constrained from 0 to 50 cm based on soils and geomorphology

### Notes on TCN approach

We utilize the inheritance concentration determined from sand samples in the modeled depth profile (Table DR3.3 and Table DR3.5) to also account for the inherited concentrations of the three desert pavement pebble samples from other terrace treads. The pavement ages were calculated using the CRONUS Calculator using the average of four scaling methods that adjust the site production rate for temporal changes in the geomagnetic field (Balco et al., 2008; Table DR3.4). The terrace surfaces have undoubtedly experienced some overall erosion since their abandonment. However, we believe the net total erosion is low for the sampled desert pavements based on: (i) unexhumed progressions of soil horizons with depth, (ii) well developed desert pavements with 1-3 cm Av horizons, and (iii) the flatness of the surface in the vicinity of the sample sites. Furthermore, desert pavement clasts are believed to remain at the surface despite erosion or dissolution of the soil over time. Thus, although our reported pavement surface ages determined with zero erosion rates are minima, we suggest they are reasonably close to the correct age. In the well constrained sand depth-profile, the most probable modal and Bayesian erosion rate is 0.38 cm/ka. We provide hypothetical results for the pavement samples adopting this modeled erosion rate estimate (Table DR3.4). These resultant ages are notably too old relative to more numerous OSL depositional age constraints, suggesting that the effective surface erosion rates of the pebble pavements are significantly less than the sand profile with depth. The methodology and results of the depth profile age, inheritance, and erosion rate calculations were previously described in detail by Hidy et al. (2010), but are reported here using a geomagnetic field corrected production rate (Table DR3.5).

# Lee's Ferry Depth Profile Calculator Output

Figure DR3.1. Matlab Input GUI (Hidy et al., 2010) for sample profile LF-404s (sand)

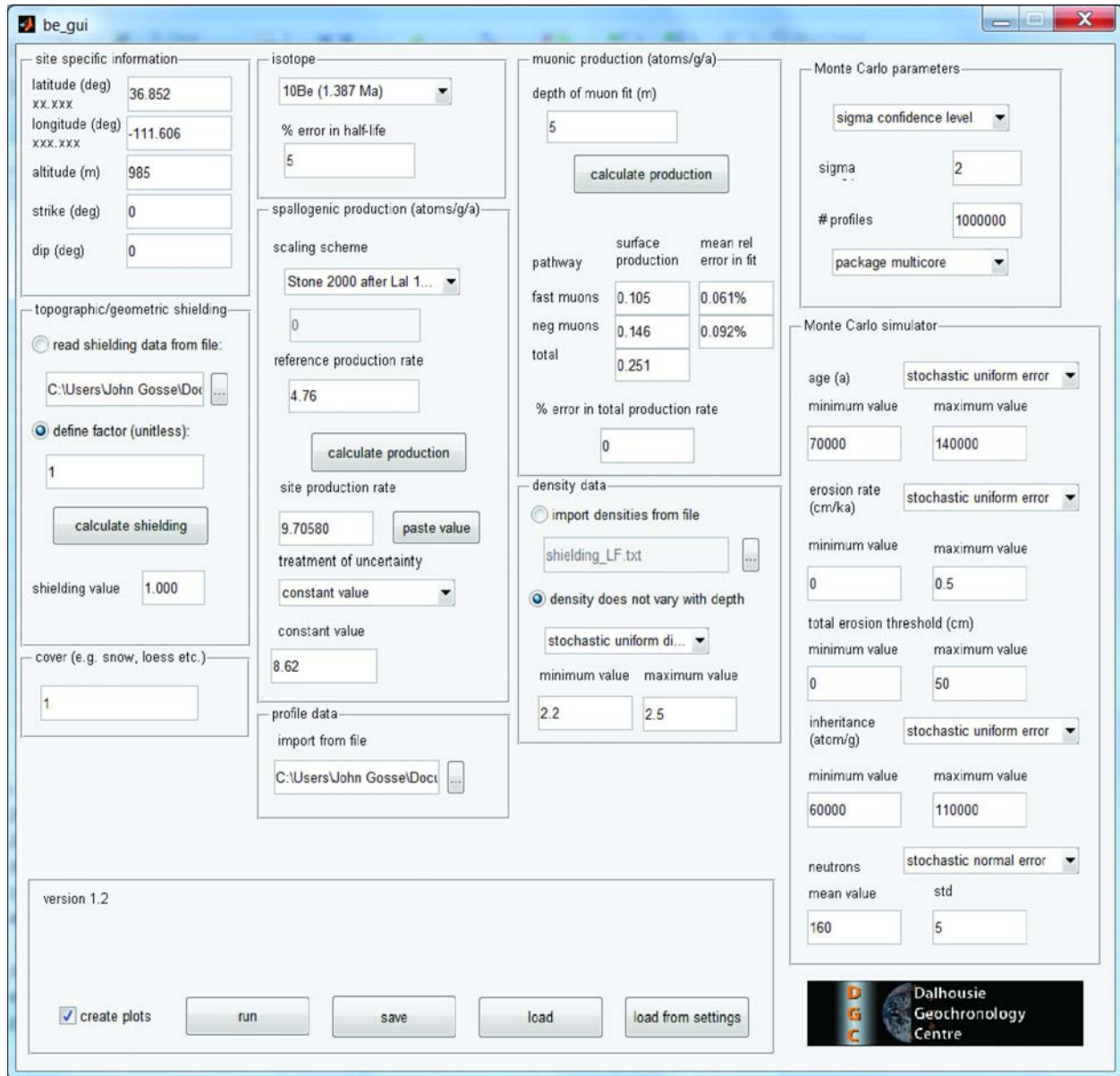


**Figure DR3.2.** Concentration vs. Depth. Graph shows all 1 million curves that fit within  $2\sigma$  of each sample concentration.

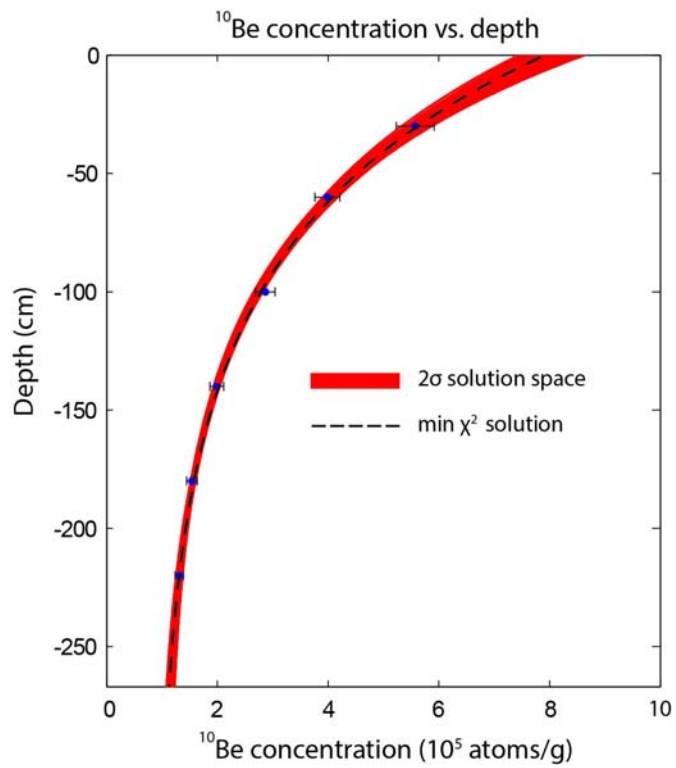


**Figure DR3.3.** Age vs. Erosion rate for depth profile LF-404sand

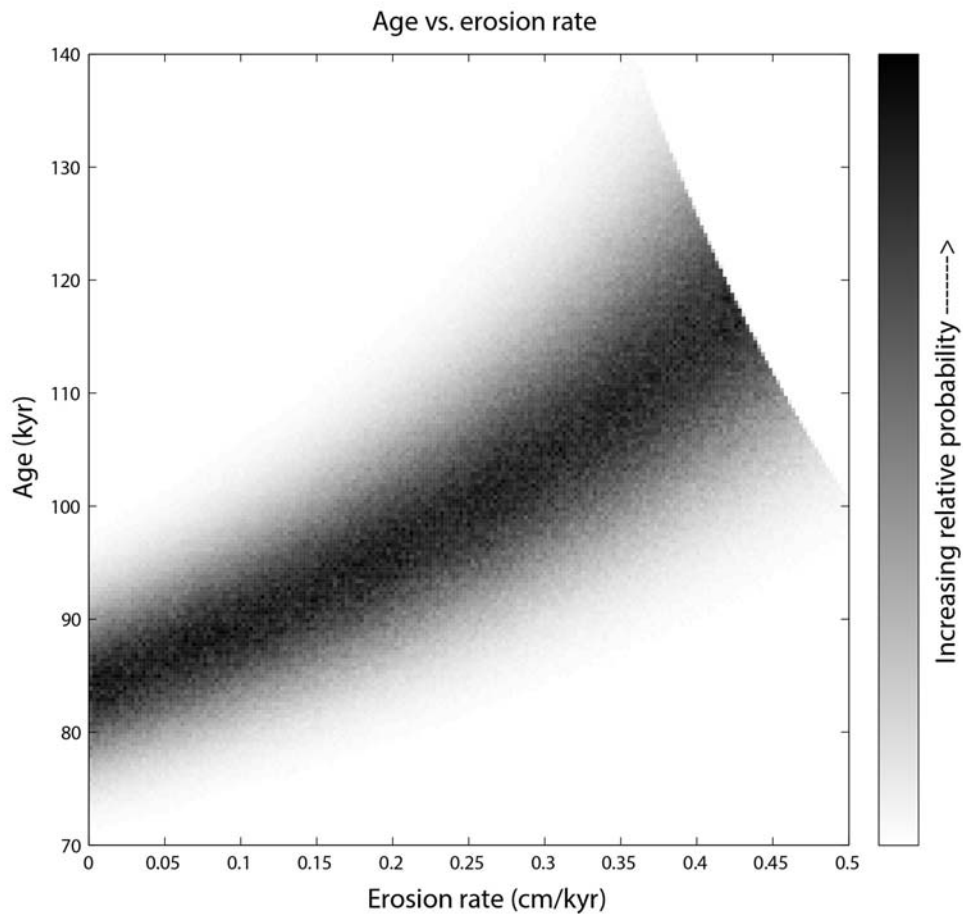
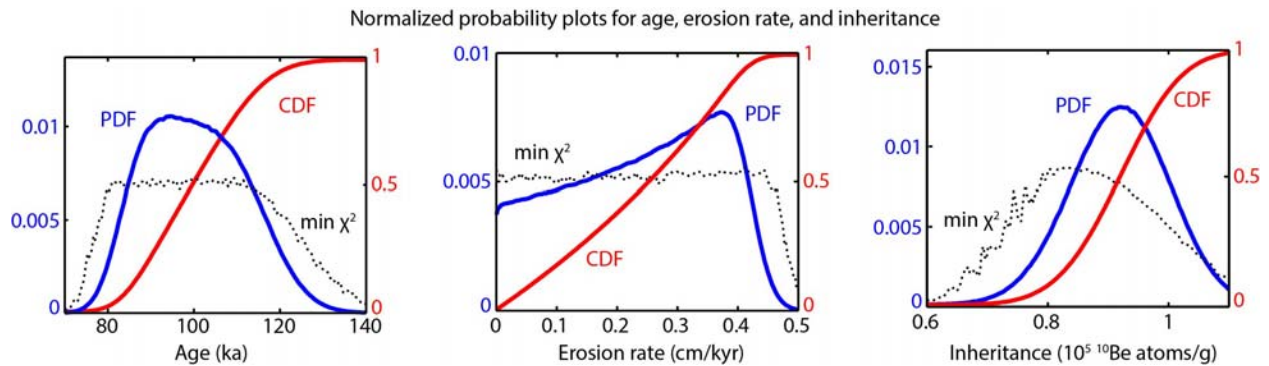


**Figure DR3.4.** Probability density function (PDF), cumulative distribution function (CDF), and minimum chi-squared ( $\min \chi^2$ ) curves for LF-404s (sand profile) for Exposure Age, Erosion Rate, and Inherited Concentration. The PDF and  $\min \chi^2$  curves are normalized such that the area under them is equal to 1.



## REFERENCES CITED

- Balco, G., Stone, J. O., Lifton, N. A., and Dunai, T. J., 2008, A complete and easily accessible means of calculating surface exposure ages or erosion rates from  $^{10}\text{Be}$  and  $^{26}\text{Al}$  measurements: *Quaternary Geochronology*, v. 3, no. 3, p. 174-195.
- Hidy, A. J., Gosse, J. C., Pederson, J. L., Mattern, J. P., and Finkel, R. C., 2010, A geologically constrained Monte Carlo approach to modeling exposure ages from profiles of cosmogenic nuclides: An example from Lees Ferry, Arizona: *Geochem. Geophys. Geosyst.*, v. 11, p. Q0AA10.
- Nishiizumi, K., Imamura, M., Caffee, M. W., Southon, J. R., Finkel, R. C., and McAninch, J., 2007, Absolute calibration of  $^{10}\text{Be}$  AMS standards: *Nuclear Instruments and Methods in Physics Research Section B: Beam Interactions with Materials and Atoms*, v. 258, no. 2, p. 403-413.